PCCP

PAPER

View Article Online
View Journal | View Issue

Cite this: *Phys. Chem. Chem. Phys.*, 2015, **17**, 14215

Predicting the degree of aromaticity of novel carbaporphyrinoids†

Rashid R. Valiev,*[ad] Heike Fliegl*[b] and Dage Sundholm*[c]

Received 5th March 2015,
Accepted 20th April 2015

DOI: 10.1039/c5cp01306b

www.rsc.org/pccp

Magnetically induced current densities have been calculated for dioxaporphyrin, dithiaporphyrin, true carbaporphyrins, and N-confused porphyrins using the gauge-including magnetically induced current (GIMIC) method. The current-strength susceptibilities (current strengths) have been obtained by numerically integrating the current flow passing selected chemical bonds. The current strength calculations yield very detailed information about the electron delocalization pathways of the molecules. The strength of the ring-current that circles around the porphyrinoid macroring is used to estimate the degree of molecular aromaticity. The studied porphyrinoid structures have been obtained by replacing the NH and N groups of porphin with formally isoelectronic moieties such as O, S, CH and CH_2. Replacing an NH moiety of *trans*-porphin with isoelectronic O and S does not significantly change the current strengths and pathways, whereas substitution of N with an isoelectronic CH group leads to significant changes in the current pathway and current strengths. CH_2 groups cut the flow of diatropic currents, whereas in strongly antiaromatic molecules a significant fraction of the paratropic ring-current is able to pass the sp^3 hybridized inner carbons. N-confused porphyrinoids sustain a ring current whose strength is about half the ring-current strength of porphin with the dominating current flow along the outer pathway *via* the NH moiety. When no hydrogen is attached to the inner carbon of the inverted pyrrolic ring, the current prefers the inner route at that ring.

1 Introduction

True carbaporphyrins are porphyrinoid molecules with one of the pyrrolic rings replaced by a five-membered all-carbon ring.[1] Such molecules were proposed more than 70 years ago by Aronoff, Calvin and Pauling,[2,3] whereas it lasted 50 years until the first true carbaporphyrins were synthesized by Berlin and Lash *et al.*[4,5] Berlicka *et al.*, Szyszko *et al.* and Lash *et al.* have more recently synthesized a variety of true carbathiaporphyrins and metal complexes of true carbaporphyrins.[1,6–9] They characterized the carbaporphyrinoids computationally and experimentally by using NMR spectroscopy and density functional theory calculations. N-confused porphyrins, which are porphyrinoids with at least one N-confused (inverted) pyrrolic ring also belong to the class of carbaporphyrins.[10,11] Carbaporphyrinoids consisting of at least one all-carbon ring are often distinguished from N-confused porphyrins by using the prefix true in front of the name of the carbaporphyrin.

The scientific community is becoming more and more interested in studies of carbaporphyrinoids because of their potential use as catalysts and their anticipated ability to form complexes with metals in unusual oxidation states.[1,8,10] The aromatic character of carbaporphyrins is also of interest, because it is assumed to be responsible for many of their molecular properties, which can be related to the number of π electrons in their conjugation network. The degree of aromaticity can to some extent be estimated by measuring ^{1}H NMR chemical shifts, whereas detailed information about the aromaticity and aromatic pathways can only be obtained computationally. The trends of the aromatic properties of true carbaporphyrins have not yet been elucidated, because only few compounds have been synthesized and reported computational studies are also rare.[1,12–14] We recently calculated magnetically induced current densities of the carbathiaporphyrins synthesized by Berlicka *et al.*[1,14] Accurate current densities were obtained in the calculations using the gauge including magnetically induced current (GIMIC) method. The current strength susceptibilities were obtained by numerical integration of the current flow passing selected chemical bonds leading to a very detailed picture of the aromatic pathways.[15–17]

[a] *Tomsk State University, Lenina 36, Tomsk, Russian Federation. E-mail: valievrashid@mail.ru*
[b] *Centre for Theoretical and Computational Chemistry (CTCC), Department of Chemistry, University of Oslo, P. O. Box 1033 Blindern, 0315 Oslo, Norway. E-mail: heike.fliegl@kjemi.uio.no*
[c] *Department of Chemistry, FIN-00014 University of Helsinki, P. O. Box 55 (A.I. Virtanens plats 1), Finland. E-mail: dage.sundholm@helsinki.fi*
[d] *Tomsk Polytechnic University, 43a Lenin Avenue, Building 2, Tomsk 634050, Russian Federation*

† Electronic supplementary information (ESI) available: The optimized Cartesian coordinates and the calculated NMR shielding constants of the studied molecules. See DOI: 10.1039/c5cp01306b

The degree of aromaticity was estimated from the strength of the ring current circling around the porphyrinoid macroring. The obtained current strength susceptibilities showed that the synthesized carbathiaporphyrins are almost as aromatic as porphins according to the ring-current criterion.[14,18,19] The current pathways were determined by calculating the current strengths along the inner and outer routes at each of the five-membered rings.[14] The GIMIC method has previously been employed in studies of the aromatic character and electron-delocalization pathways of complex planar and twisted multiring molecules.[19–26] The approach has also been successfully employed in detailed aromaticity studies of porphyrinoid molecules.[14,18,27–30]

Current density maps calculated using the ipsocentric CTOCD-DZ method have also been used for determining current pathways in porphyrins.[31–35] The ipsocentric CTOCD-DZ method employing ordinary perturbation-independent basis sets does not yield gauge-independent current densities and requires therefore large basis sets when calculating explicit current strengths.[36] The current densities obtained in CTOCD-DZ calculations can easily be decomposed into orbital contributions.[37] The current pathway in porphyrins has also been studied using nucleus independent chemical shift (NICS) calculations combined with calculations of the anisotropy of the induced current density (ACID).[38]

In this work, we perform GIMIC calculations on a number of carbaporphyrins that have not yet been synthesized. The aim of this study is to elucidate whether it is possible to obtain general trends in the aromatic properties and current pathways of the carbaporphyrins. The studied molecules are constructed by systematically modifying the structure of the porphyrinoid ring. The calculations predict relative stabilities and aromatic pathways, which might inspire organic chemists to synthesize some of the compounds.

This paper is organized as follows. The computational methods and the optimized molecular structures of the studied molecules are presented in Sections 2 and 3, respectively. The relative energies of the isomers are compared in Section 4. The results of the current density calculations are discussed for the individual molecules in Section 5. The main conclusions of the study are drawn in Section 6.

2 Computational methods

The molecular structures were optimized at the B3LYP density functional theory (DFT) level[39,40] using Turbomole 6.5.[41,42] We employed Karlsruhe triple-ζ quality basis sets (def2-TZVP).[43,44] The nuclear magnetic shieldings were calculated at the B3LYP/def2-TZVP level using Turbomole and are given in the ESI.†[45,46] The magnetically induced current densities were calculated at the same level of theory using the GIMIC program,[15–17] which is a free-standing program to calculate current densities. GIMIC uses the atomic orbital density matrix, the first-order magnetically perturbed density matrices and basis-set information as input data.[15,16] The density matrices are obtained from nuclear magnetic shielding calculations. Gauge independence and a fast basis-set convergence are obtained in the current–density calculations, because gauge-including atomic orbitals (GIAOs) are employed.[47,48]

Current strengths and pathways were obtained by performing numerical integration of the current flow passing through selected cut planes across chosen chemical bonds. The integration yields explicit values for the current–density susceptibilities (in nA T^{-1}). For simplicity, the current–density susceptibility is called current strength in the rest of the paper. The current pathways and molecular structures were plotted using ChemCraft version 1.7.[49]

3 Structures and nomenclature of the studied compounds

The aim of the present study is to investigate whether it is possible to obtain general trends in the aromaticity and current pathways for carbaporphyrins. To achieve this, we have systematically modified the molecular structure of the porphyrinoids. For the construction of the molecules, we have used the fact that CH is isoelectronic to N and that CH_2 can be considered isoelectronic to NH, O and S. Thus, it is possible to study how exchanging the heteroatoms affects the current strengths and how changes in the formal number of electrons influence molecular aromaticity.

The molecular structure of *trans*-porphin is shown in Fig. 1. It can be considered to be the reference molecule for the

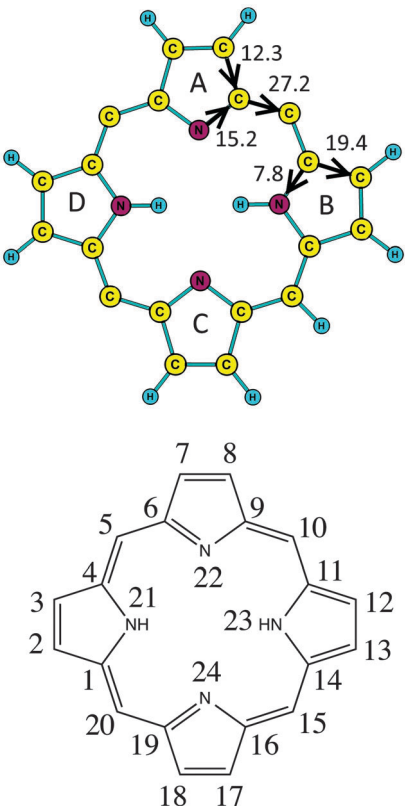

Fig. 1 (a) Calculated current strengths (in nA T^{-1}) and current pathways (arrows) for *trans*-porphin. (b) The employed numbering of the atoms for assigning names for the studied molecules.

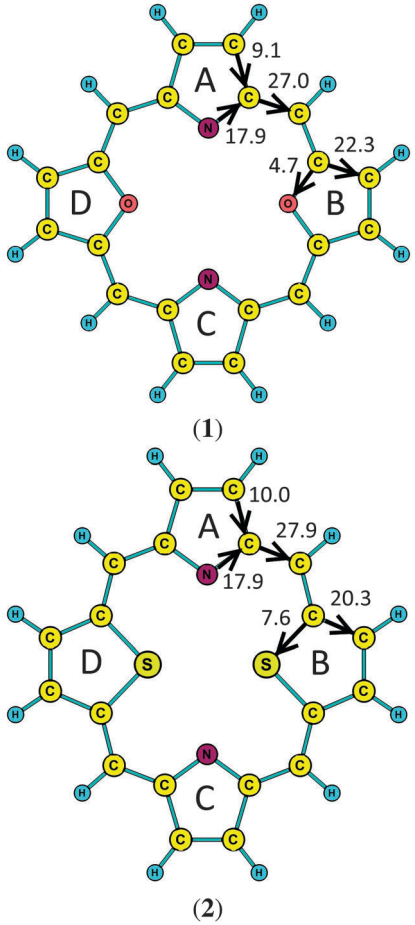

Fig. 2 Calculated current strengths (in nA T^{-1}) and current pathways (arrows) for 21,23-dioxaporphyrin (**1**) and 21,23-dithiaporphyrin (**2**).

calculated current strengths as well as the starting structure for the studied molecules. The names of the investigated carbaporphyrins have been obtained using the recommended numbering for *trans*-porphin, see for example ref. 50 and Fig. 1b.

Starting from porphin, we construct 21,23-dioxaporphyrin (**1**), 21,23-dithiaporphyrin (**2**), a set of true carbaporphyrins and a set of N-confused porphyrins. The molecular structures of dioxaporphyrin (**1**) and dithiaporphyrin (**2**) are shown in Fig. 2. The dioxaporphyrin (**1**) and dithiaporphyrin (**2**) structures are obtained by replacing the two inner NH moieties of *trans*-porphin with oxygen and sulfur, respectively. Note the significant structural difference between (**1**) and (**2**). The sulfur atoms in (**2**) seem to attract each other directly or *via* the nitrogens leading to a short S–S distance of 3.06 Å as compared to the O–O distance in (**1**) of 4.23 Å. The bond lengths of (**1**) and (**2**) are almost the same except for the S–C and O–C distances. The Cartesian coordinates are given in the ESI.†

In 22,24-*H*-21,23-dicarbaporphyrin (**3**), the inner nitrogen atoms of *trans*-porphin are replaced with CH and in 21,23-*H*-tetracarbaporphyrin or quatyrin (**4**), the two NH moieties are replaced by CH_2. In 21,22,23,24-*H*-tetracarbaporphyrin or quaternene (**5**), all inner N and NH moieties have been replaced by CH_2 by formally adding two electrons. In 2,12,22,24-*H*-tetracarbaporphyrin (**6**), the NH moieties of *trans*-porphin are replaced with CH_2 and inverted, whereas in 21,22,23,24-*H*-21,23-dicarbaporphyrin (**7**), the two inner N moieties are replaced with CH_2, which increases the formal number of electrons by two. The molecular structures of all investigated true carbaporphyrins are shown in Fig. 3 and the Cartesian coordinates are given in the ESI.† In the first set of model compounds, the formal number of electrons is unaltered as compared to *trans*-porphin (**1–4**), whereas (**5–7**) have two electrons more.

Fig. 4 shows the investigated N-confused porphyrins. 2,24-*H*-2-Azaporphyrin (**8**) can be constructed from *cis*-porphin by inverting one pyrrolic ring containing an NH group, while 2,21-*H*-2-azaporphyrin (**9**) is obtained by shifting the inner NH hydrogen of (**8**) to the CH group pointing to the inside forming a CH_2 moiety. In 2,22,24-*H*-21-dehydro-2-azaporphyrin (**10**), one of the pyrrolic rings of *trans*-porphin without an inner H is inverted and the H of the inner C is then moved to the outer N of the same pyrrolic ring. In 2,12,22,24-*H*-21,23-dehydro-2,12-diazaporphyrin (**11**), the same procedure has been employed for both pyrrolic rings without an inner H. In 2,12-*H*-2,12-diaza-dicarbaporphyrin (**12**), the two pyrrolic rings with inner hydrogens have been inverted. In the second set of model compounds, the total number of electrons is unchanged as compared to porphin, while the number of inverted rings as well as the position of the inner NH and CH tautomeric protons has been swapped. The Cartesian coordinates are given in the ESI.†

4 Relative energies

Molecules (**8**)–(**11**) are isomers of *trans*-porphin, which is the energetically lowest one. The *cis* tautomer lies 8.7 kcal mol^{-1} above *trans*-porphin. By comparing the energy of (**8**) with *cis*-porphin, one sees that an energy of 20 kcal mol^{-1} is required when inverting a pyrrolic ring. Calculations of (**3**) and (**12**) show that the energy of the inversion of pyrrolic rings is additive. Thus, the inversion of two pyrrolic rings costs 40 kcal mol^{-1}. By comparing the energy for inverting a pyrrolic ring with the difference in the energies of *trans*-porphin and (**10**), one sees that it costs 33 kcal mol^{-1} to move a H from the inner C to the outer N of the inverted pyrrolic ring. The relative energy of (**11**) with respect to *trans*-porphin shows that inverting two pyrrolic rings and moving two hydrogens from the inner C to the outer N cost 114 kcal mol^{-1}, which is slightly more than twice the energy for one such structural modification. The energy difference of 26.5 kcal mol^{-1} between (**8**) and (**9**) corresponds to the energy for moving an H from an inner NH moiety to an inner CH forming an inner CH_2. The energy between (**8**) and (**10**) of 23.1 kcal mol^{-1} is the energy needed for moving an H from an inner C to inner N. The relative energies of the N-confused porphyrins (**8**) to (**11**) with respect to *trans*-porphin and the relative energy of (**12**) with respect to (**3**) are summarized in Fig. 4.

5 Current density calculations

The calculated ring-current susceptibilities passing selected bonds and the current pathways for the studied porphyrinoids

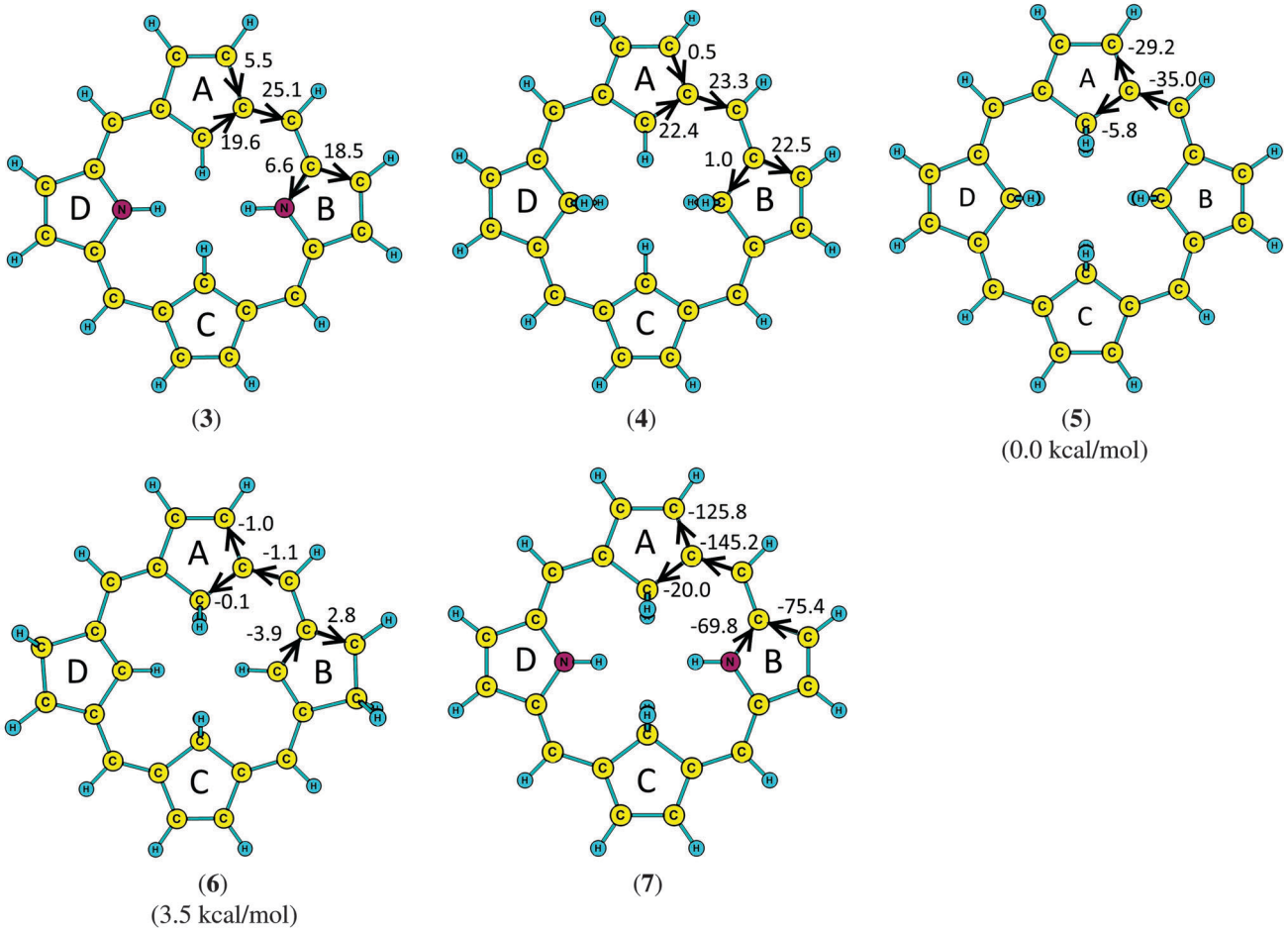

Fig. 3 Calculated current strengths (in nA T^{-1}) and current pathways (arrows) for the true carbaporphyrins 22,24-*H*-21,23-dicarbaporphyrin (**3**), 21,23-*H*-tetracarbaporphyrin or quatyrin (**4**), 21,22,23,24-*H*-tetracarbaporphyrin or quaternene (**5**), 2,12,22,24-*H*-tetracarbaporphyrin (**6**) and 21,22,23,24-*H*-21,23-dicarbaporphyrin (**7**). The relative energy difference in (kcal mol^{-1}) between (**5**) and (**6**) is also reported.

are shown in Fig. 2–4. The pathways are indicated by black arrows and the current strengths are given in nA T^{-1}. Diatropic currents are assumed to be positive and circle clockwise, whereas the anti-clockwise negative currents are paratropic. Kirchhoff's charge conservation law is largely fulfilled, except for some small discrepancies of <0.2 nA T^{-1}, which are due to the numerical integration procedure and the employed basis sets. The current pathways and current strengths for *trans*-porphin are used as references, see Fig. 1 and ref. 18.

5.1 Dioxa- and dithiaporphyrin

Dioxaporphyrin (**1**) sustains a net ring-current strength of 27.0 nA T^{-1}. Dithiaporphyrin (**2**) is the corresponding molecule with oxygen being replaced by sulfur. Dithiaporphyrin sustains a ring current of 27.9 nA T^{-1} around the porphyrin ring. The ring-current strengths of (**1**) and (**2**) are about as large as for porphin. Thus, the degree of aromaticity is not significantly affected by exchanging the inner NH moieties to the formally isoelectronic O and S, respectively. The individual five-membered rings do not sustain any ring current of their own. The ring-current flow is split into an inner and outer route at each of the five-membered rings and the current flow joins again on the other side of the ring. At the pyrrolic rings A and C, the current strength is 17.9 nA T^{-1} along the inner route, which is 2.7 nA T^{-1} stronger than that for the corresponding pathway of *trans*-porphin, whereas the currents of 9.1 nA T^{-1} and 10.0 nA T^{-1} passing the β carbons are 2–3 nA T^{-1} weaker than for *trans*-porphin. At the furan and thiophene rings (rings B and D), most of the current flow pass the β carbons. The strength of the currents passing the inner O and S is only 4.7 nA T^{-1} and 7.6 nA T^{-1}, respectively. Thus, the current pathways and current strengths of dioxaporphyrin and dithiaporphyrin are rather similar to those of *trans*-porphin. When the remaining inner N atoms are replaced with O or S, the number of π electrons increases by two leading to antiaromatic isophlorins, which we have recently studied.[27]

5.2 True carbaporphyrins

Dicarbaporphyrin (**3**), which is obtained from *trans*-porphin by replacing N with the isoelectronic CH groups, sustains a net ring current of 25.1 nA T^{-1}. Thus, according to the ring-current criterion it is only 8% less aromatic than porphin. The current

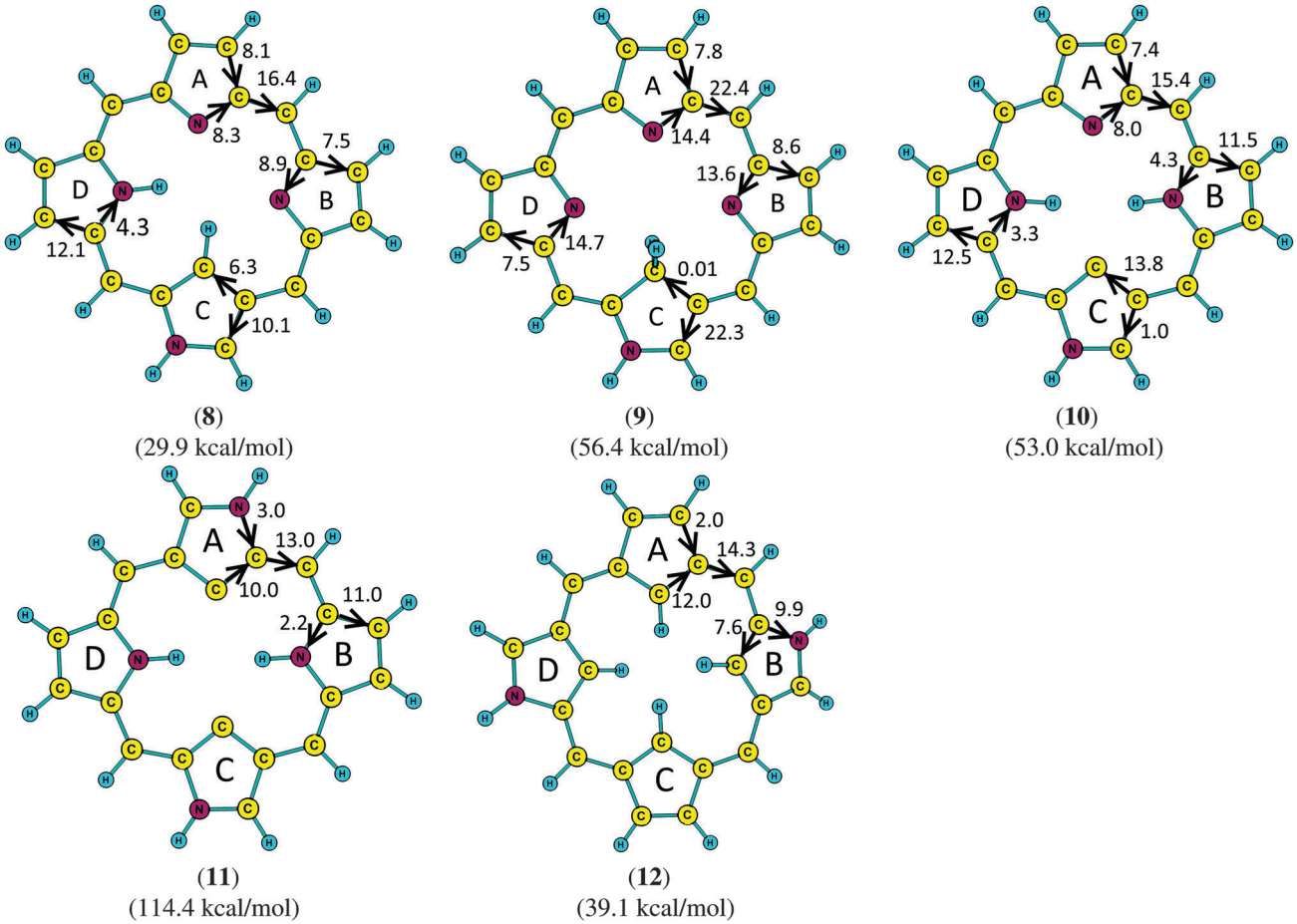

Fig. 4 Calculated current strengths (in nA T^{-1}) and current pathways (arrows) for the N-confused porphyrins 2,24-*H*-2-azaporphyrin (**8**), 2,21-*H*-2-azaporphyrin (**9**), 2,22,24-*H*-21-dehydro-2-azaporphyrin (**10**), 2,12,22,24-*H*-21,23-dehydro-2,12-diazaporphyrin (**11**) and 2,12-*H*-2,12-diazadicarbaporphyrin (**12**). For (**8**)–(**11**), the relative energies (in kcal mol^{-1}) with respect to *trans*-porphin are reported. For comparison, *cis*-porphin lies 8.7 kcal mol^{-1} above *trans*-porphin. The energy of (**12**) relative to (**3**) is also given.

density calculations show that the current pathway of (**3**) is qualitatively the same as the one for *trans*-porphin. At all carbon five-membered rings (rings A and C), a current of 19.6 nA T^{-1} passes the inner CH unit, which is 4.4 nA T^{-1} stronger than for the corresponding ring of *trans*-porphin. Thus, the substitution of N with CH leads to a stronger current along the inner pathway. For rings B and D, the ratio between the current flow along the inner and outer route is almost the same as for *trans*-porphin. Even though the bond-length alternation in ring A is rather large with bond lengths 1.35 Å, 1.47 Å and 1.41 Å for C_β–C_β, C_α–C_β and C_α–C_{inner}, respectively, rather strong currents pass all bonds of the ring. Ring B does not differ much from the corresponding ring of porphin. The C_β–C_β and C_α–C_β distances in porphin are 1.37–1.38 Å and 1.44–1.47 Å, respectively.

Tetracarbaporphyrin (**4**), which is obtained by substituting the inner NH group of rings B and D of (**3**) with the isoelectronic CH_2, is aromatic with a net ring-current strength of 23.3 nA T^{-1}. The inner CH_2 groups almost prevent the current flow along that way, only 1.0 nA T^{-1} passes the saturated inner carbon atom. A current flow of 0.5 nA T^{-1} along the outer pathway of rings A and C is even smaller. The C_β–C_β bond of ring A is short, whose length is 1.35 Å which is typical for a C=C double bond. For ring B, the length of the inner C–C bonds is 1.50 Å. Thus, (**4**) is an 18π porphyrinoid with pronounced inner and outer pathways at rings A (C) and B (D), respectively.

Tetracarbaporphyrin (**5**) has been constructed by replacing all N and NH moieties on the inside of the macroring by CH_2 implying that formally two electrons have been added. Since the added electrons lead to a change from aromatic to antiaromatic, (**5**) follows Hückel's $4N$ π-electron rule for antiaromaticity. (**5**) sustains a strong net paratropic ring current of −35.0 nA T^{-1} showing that it is antiaromatic according to the magnetic criterion. The substitution of N for CH_2 yields a sp^3 hybridized carbon in the inner position of all five-membered rings. The outer pathway accommodates 20 π electrons leading to antiaromaticity. It is though remarkable that a paratropic current of −5.8 nA T^{-1} also passes the sp^3 hybridized inner carbons.

Tetracarbaporphyrin (**6**) is obtained by substituting two outer CH groups of (**4**) with CH_2. Alternatively, (**6**) can be considered as a doubly N-confused porphyrin for which both outer NH moieties have been replaced by CH_2. (**6**) has $4N$ π

electrons implying that it is not expected to be aromatic according to the Hückel π electron rule. The inner CH_2 moieties of rings A and C can be expected to prevent the current to take that route, whereas the outer CH_2 groups of rings B and D are expected to stop the current flow that way. Thus, the possible pathway of the ring current accommodates 18 π electrons, whereas the two π electrons at the β carbons of rings B and D do not belong to the expected current pathway. The nonaromatic (**6**) lies energetically 3.4 kcal mol^{-1} above the antiaromatic (**5**).

The calculated current strengths show that (**6**) is very weakly antiaromatic or practically nonaromatic sustaining a ring current of −1.1 nA T^{-1} around the porphyrinoid ring. Rings B and D are weakly aromatic sustaining a local ring current of 2.8 nA T^{-1}. The weak paratropic current takes the outer route at ring A and the inner one at ring B. Thus, the inversion and saturation destroy the aromaticity of (**6**). Even though an aromatic pathway containing 18 π electrons is formed in the porphyrinoid ring, the two extra π electrons seem to have a strong influence on the aromatic properties of (**6**). Saturating the two remaining sp^2 hybridized outer carbons of rings B and D in (**6**) would most likely lead to an aromatic carbaporphyrin that is analogous to bacteriochlorin.

Dicarbaporphyrin (**7**) has two inner NH and two inner CH_2 moieties implying that it has $4N$ π electrons. Current density calculations show that (**7**) is strongly antiaromatic sustaining a paratropic ring current of −145.2 nA T^{-1} around the porphyrinoid ring, which is the strongest paratropic ring current that we have so far obtained for any porphyrinoid molecule. At rings B and D with the inner NH group, the ring current is almost equally split between the inner and outer routes, whereas for rings A and C, most of the current takes the outer route.

The outer periphery of (**7**) accommodates 20 π electrons. The outer and the inner pathways of the two pyrrolic rings (B and C) have 4 π electrons implying that several pathways with 20 π electrons can be constructed. The same formally holds for rings A and C. However, the sp^3 hybridized inner carbons prevent most of the current flow to take that route. However, even though only a small fraction of the total ring current passes the inner carbons, the strength of the paratropic current passing the sp^3 hybridized inner carbons is −20 nA T^{-1}. Thus, strong currents are hard to stop as long as there are electrons that can transport them.

5.3 N-confused porphyrins

The N-confused porphyrin (**8**) can be constructed by inverting one of the pyrrolic rings of *cis*-porphin with an inner H. (**8**) is a common starting point for the synthesis of N-confused porphyrinoids, because (**8**) is easily synthesized having three sites of different reactivity on the inverted pyrrolic ring.[12,51–53] The inversion of the pyrrolic ring leads to a decrease in the net current strength of the molecule from 27.0 nA T^{-1} (*cis*-porphin) to 16.4 nA T^{-1}.[18] However, (**8**) is still aromatic according to the ring-current criterion. As for *cis*-porphin and *trans*-porphin, the current is almost equally divided between the inner and outer pathways at rings A and B that have no inner hydrogen, whereas at ring D the current mainly flows on the outside along the C–C bond as also observed for the inverted ring C, where 10.1 nA T^{-1} passes the outer NH group and 6.3 nA T^{-1} takes the inner pathway. The ratio between the current strengths of the inner and outer route for rings A, B and D is the same as for the corresponding ring of *trans*-porphin. The calculations show that the resistance of the NH group of porphyrins is larger than for N, which has also been obtained in previous studies.[15,18] Thus, the outer NH group reduces the current flow along the outer route, which is the preferred current pathway leading to a smaller ring current around the porphyrinoid ring.

The N-confused porphyrin (**9**) has an inner CH_2 of the inverted pyrrolic ring C. The current density calculations show that the sp^3 hybridized inner carbon prevents the current to take that route. However, the net ring-current strength around the porphyrinoid ring of 22.4 nA T^{-1} is 6 nA T^{-1} larger than for (**8**) but 5 nA T^{-1} weaker than for *trans*-porphin. At rings A, B and D, the current is split into a stronger current of 13.6–14.7 nA T^{-1} along the inner pathway, whereas 7.5–8.6 nA T^{-1} takes the outer route.

The N-confused porphyrin (**10**) consists of one inverted pyrrolic ring with the NH moiety pointing outwards with no H attached to the inner C of that ring. The rest of the *trans*-porphin motif remains unaltered. (**10**) is aromatic with a net current strength of 15.4 nA T^{-1}, which is almost half the ring current of *trans*-porphin. The current is almost equally split at the pyrrolic ring without an inner H (ring A), whereas at rings B and D the current prefers the outer route. A current of only 3.3–4.3 nA T^{-1} passes the inner NH moieties. At the inverted pyrrolic ring, the current takes almost entirely the inner route with a current strength of 13.8 nA T^{-1} as compared to 1.0 nA T^{-1} along the outer pathway.

Two pyrrolic rings without inner H have been inverted in (**11**) and hydrogens connected to the inner carbons are moved to the outer nitrogens, which leads to a very high-energy isomer. The net current around the porphyrinoid ring is 13.0 nA T^{-1}, which is 2 nA T^{-1} weaker than for (**10**), which has only one inverted pyrrolic ring. As expected, the main current flows along the inner route at the inverted pyrrolic rings and takes the outer one at the two other pyrrolic rings.

The N-confused porphyrin (**12**) is the doubly inverted dicarbaporphyrin (**3**). The net ring current of (**12**) is 14.3 nA T^{-1}, which is about the same as obtained for (**10**) and (**11**) and about half the ring current for (**3**) and *trans*-porphin. At the inverted rings, the current is almost equally divided between the outer and inner routes with a somewhat stronger current along the outer pathway. The current along the inner pathway at the all-carbon five-membered rings is six times stronger than along the outer one.

6 Conclusions

Magnetically induced current densities have been calculated for a set of true carbaporphyrins and N-confused porphyrins with the aim to elucidate how the currents flow around the porphyrinoid macroring and what kind of factor affects the current pathways and the strengths of the ring currents. The reference compounds of this study are *trans*-porphin and *cis*-porphin, whose current strengths and aromatic pathways

have previously been studied in detail.[18] The porphyrinoid structure has been systematically modified by replacing NH and N at the pyrrolic rings with isoelectronic moieties such as O, S, CH and CH_2. Even though CH_2 is formally isoelectronic with NH, O and S, it does not contribute to the number of π electrons of the porphyrinoid ring. Instead, it cuts the conjugation pathway of the molecule, thereby altering the number of π electrons in the electron delocalization pathway. The calculations show that the CH_2 groups cut the flow of diatropic currents, whereas in strongly antiaromatic molecules such as (**5**) and (**7**), a large fraction of the paratropic ring current passes the sp^3 hybridized inner carbon.

This study shows that replacing the NH moiety of *trans*-porphin with isoelectronic atoms such as O or S does not significantly change the current strengths and pathways, whereas by replacing the inner N with an isoelectronic CH group leads to significant changes in the current pathway and current strengths. The substitution leads to a stronger current *via* the inner CH group than *via* N in *trans*-porphin, whereas the total current of (**3**) is only 2 nA T^{-1} weaker than for *trans*-porphin.

When the inner and NH and N moieties are replaced by CH_2, the porphyrinoids have formally 20 π electrons implying that they are antiaromatic. The inner CH_2 prevents the current flow in (**5**) yielding an antiaromatic outer periphery of the porphyrinoid. When two of the CH_2 are in the outer periphery and two are on the inside of the two other five-membered all-carbon rings, the only possible ring-current pathway passes 18 carbons with one π electron each. Two of the 20 π electrons lie on carbon atoms outside the ring-current pathway. Thus, molecule (**6**) has 20 π electrons of which 18 can be involved in the aromatic pathway. The conflict between Hückel aromaticity and antiaromaticity leads to a nonaromatic porphyrinoid.

Inversion of a pyrrolic ring generally leads to a significant weakening of the ring current around the porphyrinoid ring. The ring-current strength of (**8**) of 16.4 nA T^{-1} is slightly larger than half the current strength of *trans*-porphin. The inversion of the pyrrolic ring directs more current to the inner pathway of the inverted pyrrolic ring. Inversion of two pyrrolic rings does not lead to an additional weakening of the ring current strength as seen from the comparison of the current strengths of (**8**) and (**12**).

The present study shows how current density calculations using the GIMIC method can be used to assess changes in the current strengths and the current pathway due to the modification of different molecular moieties. The calculations show that porphyrinoids with $(4N + 2)$ π electrons in most cases maintain their aromatic properties, even though substitutions generally reduce the current strengths. Molecules with $4N$ π electrons are antiaromatic except when all π electrons cannot participate in the current transport around the ring, which in this study lead to a nonaromatic porphyrinoid.

Acknowledgements

This work has been supported by the Academy of Finland through the Computational Science Research Programme LASTU (258258) and by its projects (137460 and 266227). We thank the Norwegian Research Council for financial support through the CoE Centre for Theoretical and Computational Chemistry (Grand No. 179568/V30 and 231571/F20) and Magnus Ehrnrooth foundation for a grant. The computational resources have been provided by CSC – the Finnish IT Center for Science – and by the Norwegian Supercomputing Program NOTUR (Grant No. NN4654K).

References

1 A. Berlicka, P. Dutka, L. Szterenberg and L. Latos-Grażyński, *Angew. Chem., Int. Ed.*, 2014, **53**, 4885–4889.
2 S. Aronoff and M. Calvin, *J. Org. Chem.*, 1943, **8**, 205–223.
3 M. O. Senge, *Angew. Chem., Int. Ed.*, 2011, **50**, 4272–4277.
4 K. Berlin, *Angew. Chem., Int. Ed.*, 1996, **35**, 1820–1822.
5 T. D. Lash and S. T. Chaney, *Chem. – Eur. J.*, 1996, **2**, 944–948.
6 B. Szyszko, L. Latos-Grażyński and L. Szterenberg, *Angew. Chem., Int. Ed.*, 2011, **50**, 6587–6591.
7 T. D. Lash, M. J. Hayes, J. D. Spence, M. A. Muckey, G. M. Ferrence and L. F. Szczepura, *J. Org. Chem.*, 2002, **67**, 4860–4874.
8 T. D. Lash, *Eur. J. Org. Chem.*, 2007, 5461–5481.
9 D. I. AbuSalim and T. D. Lash, *J. Org. Chem.*, 2013, **78**, 11535–11548.
10 M. Pawlicki and L. Latos-Grażyński, *Chem. Rec.*, 2006, **6**, 64–78.
11 A. Ghosh, *Angew. Chem., Int. Ed.*, 2004, **43**, 1918–1931.
12 D. Li and T. D. Lash, *J. Org. Chem.*, 2014, **79**, 7112–7121.
13 T. D. Lash, G. C. Gilot and D. I. AbuSalim, *J. Org. Chem.*, 2014, **79**, 9704–9716.
14 R. R. Valiev, H. Fliegl and D. Sundholm, *J. Phys. Chem. A*, 2015, **119**, 1201–1207.
15 J. Jusélius, D. Sundholm and J. Gauss, *J. Chem. Phys.*, 2004, **121**, 3952–3963.
16 S. Taubert, D. Sundholm and J. Jusélius, *J. Chem. Phys.*, 2011, **134**, 054123.
17 H. Fliegl, S. Taubert, O. Lehtonen and D. Sundholm, *Phys. Chem. Chem. Phys.*, 2011, **13**, 20500–20518.
18 H. Fliegl and D. Sundholm, *J. Org. Chem.*, 2012, **77**, 3408–3414.
19 H. Fliegl, D. Sundholm, S. Taubert, J. Jusélius and W. Klopper, *J. Phys. Chem. A*, 2009, **113**, 8668–8676.
20 S. Taubert, D. Sundholm and F. Pichierri, *J. Org. Chem.*, 2009, **74**, 6495–6502.
21 S. Taubert, J. Jusélius, D. Sundholm, W. Klopper and H. Fliegl, *J. Phys. Chem. A*, 2008, **112**, 13584–13592.
22 S. Taubert, D. Sundholm and F. Pichierri, *J. Org. Chem.*, 2010, **75**, 5867–5874.
23 M. Kaipio, M. Patzschke, H. Fliegl, F. Pichierri and D. Sundholm, *J. Phys. Chem. A*, 2012, **116**, 10257–10268.
24 H. Fliegl, D. Sundholm, S. Taubert and F. Pichierri, *J. Phys. Chem. A*, 2010, **114**, 7153–7161.
25 H. Fliegl, D. Sundholm and F. Pichierri, *Phys. Chem. Chem. Phys.*, 2011, **13**, 20659–20665.
26 D. Sundholm, *Phys. Chem. Chem. Phys.*, 2013, **15**, 9025–9028.

27 R. R. Valiev, H. Fliegl and D. Sundholm, *J. Phys. Chem. A*, 2013, **117**, 9062–9068.
28 R. R. Valiev, H. Fliegl and D. Sundholm, *Phys. Chem. Chem. Phys.*, 2014, **16**, 11010–11016.
29 H. Fliegl, N. Özcan, R. Mera-Adasme, F. Pichierri, J. Jusélius and D. Sundholm, *Mol. Phys.*, 2013, **111**, 1364–1372.
30 H. Fliegl, F. Pichierri and D. Sundholm, *J. Phys. Chem. A*, 2015, **119**, 2344–2350.
31 E. Steiner and P. W. Fowler, *Org. Biomol. Chem.*, 2002, **3**, 114–116.
32 E. Steiner and P. W. Fowler, *Org. Biomol. Chem.*, 2004, **2**, 34–37.
33 E. Steiner, A. Soncini and P. W. Fowler, *Org. Biomol. Chem.*, 2005, **4**, 4053–4059.
34 E. Steiner and P. W. Fowler, *Org. Biomol. Chem.*, 2006, **4**, 2473–2476.
35 E. Steiner, P. W. Fowler, A. Soncini and L. W. Jenneskens, *Faraday Discuss.*, 2007, **135**, 309–323.
36 R. Carion, B. Champagne, G. Monaco, R. Zanasi, S. Pelloni and P. Lazzeretti, *J. Chem. Theory Comput.*, 2010, **6**, 2002–2018.
37 G. Monaco, R. Zanasi, S. Pelloni and P. Lazzeretti, *J. Chem. Theory Comput.*, 2010, **6**, 3343–3351.
38 J. I. Wu, I. Fernandez and P. v. R. Schleyer, *J. Am. Chem. Soc.*, 2013, **135**, 315–321.
39 A. D. Becke, *J. Chem. Phys.*, 1993, **98**, 5648–5652.
40 C. Lee, W. Yang and R. G. Parr, *Phys. Rev. B: Condens. Matter Mater. Phys.*, 1988, **37**, 785–789.
41 R. Ahlrichs, M. Bär, M. Häser, H. Horn and C. Kölmel, *Chem. Phys. Lett.*, 1989, **162**, 165–169.
42 F. Furche, R. Ahlrichs, C. Hättig, W. Klopper, M. Sierka and F. Weigend, *Wiley Interdiscip. Rev.: Comput. Mol. Sci.*, 2014, **4**, 91–100.
43 A. Schäfer, H. Horn and R. Ahlrichs, *J. Chem. Phys.*, 1992, **97**, 2571–2577.
44 F. Weigend and R. Ahlrichs, *Phys. Chem. Chem. Phys.*, 2005, **7**, 3297–3305.
45 M. Häser, R. Ahlrichs, H. P. Baron, P. Weis and H. Horn, *Theor. Chim. Acta*, 1992, **83**, 455–470.
46 M. Kollwitz, M. Häser and J. Gauss, *J. Chem. Phys.*, 1998, **108**, 8295–8301.
47 R. Ditchfield, *Mol. Phys.*, 1974, **27**, 789–807.
48 K. Wolinski, J. F. Hinton and P. Pulay, *J. Am. Chem. Soc.*, 1990, **112**, 8251–8260.
49 G. A. Zhurko and D. A. Zhurko, http://www.chemcraftprog.com/.
50 G. P. Moss, *Eur. J. Biochem.*, 1986, **178**, 277–328.
51 B. Liu, X. Li, J. Macioek, M. Stepień and P. J. Chmielewski, *J. Org. Chem.*, 2014, **79**, 3129–3139.
52 P. J. Chmielewski and L. Latos-Grażyński, *Coord. Chem. Rev.*, 2005, **249**, 2510–2533.
53 P. J. Chmielewski, *Inorg. Chem.*, 2007, **46**, 1617–1626.

